

Bragg reflector one-dimensional multi-layer structure sensor for the detection of thyroid cancer cells

Ranjeet Kumar Pathak¹, Sumita Mishra¹, Preeti Sharan²

¹Department of ECE, Amity School of Engineering and Technology, Amity University Uttar Pradesh, Lucknow, India

²Department of ECE, The Oxford College of Engineering, Bangalore, India

Article Info

Article history:

Received Jul 09, 2022

Revised Dec 15, 2022

Accepted Dec 28, 2022

Keywords:

Bragg's reflector

Characteristic matrix method

Micro-cavity

Photonic crystal

Thyroid cancerous cells

ABSTRACT

In the proposed work, a defect cavity multi-layer Bragg reflector structure is proposed theoretically to find the presence of thyroid cancer cells in the given sample. The modelling, design and analysis of the sensor is performed using characteristic matrix method (CMM). Proposed structure has central defect cavity with 6 pairs of low and high refractive index layers on each side of the defect. To enhance the sensor sensitivity, the incident light in mid-infrared frequency range is used as input light source. The refractive index of normal and thyroid cancer cells is analysed for the performance of the sensor. The obtained Q factor and sensitivity of the sensor design is 3729 and 2828 nm/RIU respectively. The proposed sensor is a best choice of optical sensor for the detection of thyroid cancer cells in the given test sample for accurate analysis in medical applications.

This is an open access article under the [CC BY-SA](https://creativecommons.org/licenses/by-sa/4.0/) license.



Corresponding Author:

Ranjeet Kumar Pathak

Department of ECE, Amity School of Engineering and Technology

Amity University Uttar Pradesh, Lucknow, India

Email: pathak84@yahoo.co.in

1. INTRODUCTION

Thyroid, an important organ in the human body butterfly in shape and located below the Adams apple of the front neck region. It has two side lobes which is connected by isthmus [1]. Thyroid is rich in blood vessels and plays important role in voice quality. It generates various hormones which plays a significant role in the various parts of the body. Metabolism is one such process where the food digestion is converted into energy and is controlled by with the proper generation of thyroid hormones [2]. When thyroid generates too low or too high thyroid hormones, it causes hypothyroidism or hyperthyroidism respectively. The two specific and significant hormones generated by thyroid glands are thyroxine (T4) and triiodothyronine (T3) [3]. These two hormones are responsible for informing the body cells to properly utilize the energy available. In its normal working thyroid generates balanced level of these two hormones and control the body activity. The entire activity of thyroid is under the control of pituitary gland. It is located below the brain and in the center of the skull. This pituitary gland is responsible for sensing and controlling the amount of thyroid hormones in the blood stream. When pituitary gland senses the deficiency or increased amount of thyroid hormones, it automatically adjusts the hormones level by its own. This is done by generating thyroid stimulating hormone (TSH) hormones [4]. This TSH hormone instructs the thyroid gland to take some decisions to bring back the body with normal conditions. Thyroid disease is a general term used to mention the imbalanced level of thyroid hormones in the body-system. Increased thyroid hormones makes the body to consume more amount of energy too quickly. It also causes tiredness and reduction in the body weight. On counterpart, if thyroid generates too low level of hormones, the amount of energy consumed by the cells reduces and causes tiredness and makes to gain body weight. Thyroid disease may found in men,

women, teenagers, infants and elderly persons. It can be inherited and passed down through families. Hyperthyroidism can be found during the birth and may develop with the age. There are many reasons to have thyroid diseases viz, family history, anemia, type 1 diabetes, turner syndrome, with the age like more than 60. People with type 1 diabetes are more likely to get thyroid disease and compared to others as type 1 diabetes is an autoimmune disorder [5]. Symptoms of hyperthyroidism includes, anxiety, weight loss, goiter, muscle weakness, nervousness, irritability [6] and that of hypothyroidism includes, gaining weight, fatigue, forgetfulness, hoarse voice, intolerance to cold temperatures [7]. For the year 2022 The American Cancer Society estimates about 43,800 cases of thyroid cancers with around 2,230 deaths [8]. There is about 0.6% increase per year in the death rate due to thyroid cancer. Studies concludes that women's were 3 times more likely to attack for thyroid cancer than men's. Blood test, imaging and physical examinations are the commonly used test to diagnose the thyroid cancer. These examinations have limitations like more sample requirement, less accuracy, more detection time, experienced lab technicians and costlier. Micro-electro mechanical systems (MEMS), micro-opto-electro mechanical systems (MOEMS) and optical sensors plays an important role in biomedical applications [9], [10]. Optical sensors are the best choice for sensing application as they require less sample, small in size and weight, more accurate, no electromagnetic interference (EMI) and can be fabricated using micro-machining techniques [11], [12].

2. THEORETICAL DESIGN AND METHODOLOGY

Easy fabrication, simple design, quick and accurate sensing of a sample are the major factors that many researchers considered while designing sensors. The best choice to satisfy these criteria are 1D photonic crystals. By properly choosing the material used for designing the sensor, the properties of the light inside the PhC can be precisely controlled [12], [13]. Photonic band gap (PBG) is the unique property of PhC which indicates the frequency range prohibiting from the light propagation [14], [15]. By creating a defect in the structure, the light can be made to propagate in this frequency region. Structures containing stack of alternating layers of two different refractive index (RI) materials is called distributed Bragg reflector (DBR). It acts as 1D photonic crystal due to its periodic variation in the RI of the material in only one direction. As the light is incident on these structures, a part of the light is transmitted, and the remaining part is reflected. This can be observed in every boundary at the interface of two materials. Due to constructive interference, the reflected light combined and causes a very high reflection. Stopband is the frequency range where the light propagation is forbidden and hence exhibits the property of photonic bandgap [16]–[18]. Figure 1 shows the structure of 1D DBR consists of alternating layers of two different RI materials. The structure considered has $N = 6$ pairs of low (L) and high (H) RI material.

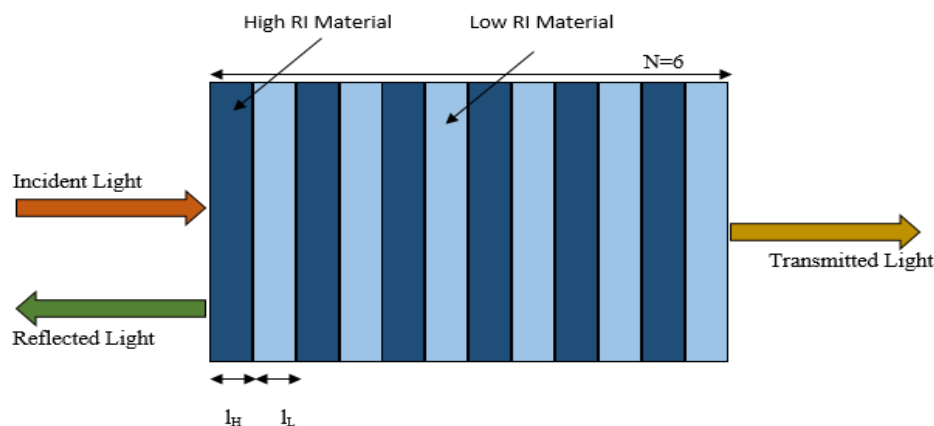


Figure 1. Proposed multi-layer DBR structure having $N = 6$

To calculate the RI value of each material we can use the following formula:

$$n_H = \sqrt{\epsilon_H}, n_L = \sqrt{\epsilon_L} \quad (1)$$

Where, n_L and n_H are the RI of low and high layer respectively with the permittivity ϵ_L and ϵ_H .

The incident electromagnetic wave experience multiple reflections as it propagates through DBR. For this multiple Bragg reflection, the optical length of each layer should be equal to the quarter wavelength of the incident light.

$$n_H l_H \cos \theta_H = n_L l_L \cos \theta_L = \frac{\lambda_0}{4} \quad (2)$$

Where, l_L and l_H indicates the geometrical thickness of layer low and high RI material respectively $\lambda_0 = \frac{2\pi c}{\omega_0}$ is the wavelength of incident light and c being the free space velocity of the electromagnetic wave. Figure 2 shows the transmission spectrum of $N = 6$ pair DBR. It is clear from the transmission spectrum that, for a certain frequency range there is no transmission. This region is called photonic band gap (PBG) region.

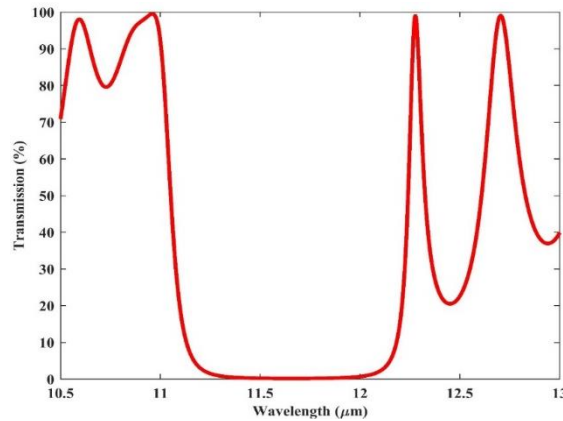


Figure 2. $N = 6$ pair multi-layer DBR structure transmission spectrum

In this work, the high RI layer (H) is made with germanium (Ge) material and the low RI layer (L) is made with zinc sulphide (ZnS) material with $RI = 4$ and $RI = 2.19$ respectively. For the devices operating in the mid-infrared wavelength range ($3 \mu\text{m} - 25 \mu\text{m}$), Ge and ZnS are the commonly chosen materials. They have the advantages of lower absorption coefficient, higher refractive index contrast and easy fabrication process. By using pumped CO₂ lasers, these devices can be operated at THz frequency ranges [19], [20]. Sol-gel and spin coating methods make the DBR fabrication easy [21]–[23]. Reactive electron beam or chemical vapor deposition (CVD) methods of deposition can also be used for the fabrication of multi-layer structures. The imaginary part of RI of the materials used here is neglected as these materials have very low absorption coefficient at the frequency range used here. For the proposed design, mid-infrared wavelength of $10.6 \mu\text{m}$ incident light is considered. Because of good molecular fingerprints in the mid-infrared region, it offers higher sensitivity of the sensor [24], [25]. The obtained geometrical thickness for low and high index layer is $1.21 \mu\text{m}$ and $0.6625 \mu\text{m}$ respectively. All the simulations were done using Matlab tool.

3. CHARACTERISTIC MATRIX METHOD

In characteristic matrix method (CMM) is used to analyse the interaction of incident electromagnetic waves with the layered media. The incident light is assumed to incident normally on the first layer and is transverse electric (TE) polarized. If the angle of incidence is denoted by θ then, for TE wave, we have [13], [26].

$$\frac{d^2 U}{dz^2} + (k_0^2 n^2 \cos^2 \theta) U = 0, \quad \frac{d^2 V}{dz^2} + (k_0^2 n^2 \cos^2 \theta) V = 0 \quad (3)$$

The solution obtained for the (3) are:

$$U(z) = A \cos(k_0 n z \cos \theta) + B \sin(k_0 n z \cos \theta)$$

$$V(z) = \frac{1}{i} \sqrt{\frac{\epsilon}{\mu}} \cos \theta \{B \cos(k_0 n z \cos \theta) - A \sin(k_0 n z \cos \theta)\}$$

The obtained characteristics matrix is:

$$M(z) = \begin{bmatrix} \cos(k_0 n z \cos \theta) & -\frac{i}{p} \sin(k_0 n z \cos \theta) \\ -ip \sin(k_0 n z \cos \theta) & \cos(k_0 n z \cos \theta) \end{bmatrix} \quad (4)$$

With, $p = \sqrt{\frac{\epsilon}{\mu}} \cos \theta$

The characteristic matrix for two layers is given as:

$$\begin{aligned} M(z_1) &= M_0(z_0)M_1(z_1 - z_0) \\ M(z_2) &= M_1(z_1)M_2(z_2 - z_1) \\ Q_0 &= M_1(z_1)Q(z_1) \end{aligned} \quad (5)$$

Where, $Q(z_1) = M_2(z_2 - z_1)Q(z_2)$.

The characteristic matrix of a j th layer is given by:

$$M_j = \begin{bmatrix} 1 & -\frac{i}{p_j} k_0 n_j \delta z_j \cos \theta_j \\ -i p_j k_0 n_j \delta z_j \cos \theta_j & 1 \end{bmatrix} \quad (6)$$

The characteristic matrix of the N layered media is given as:

$$M = \begin{bmatrix} 1 & -i k_0 B \\ -i k_0 A & 1 \end{bmatrix} \quad (7)$$

With, $A = \sum_{j=1}^N p_j n_j \delta z_j \cos \theta_j$ and $B = \sum_{j=1}^N \frac{n_j}{p_j} \delta z_j \cos \theta_j$. For an N layered media, this CMM is calculated as:

$$M = \begin{bmatrix} m_{11} & m_{12} \\ m_{21} & m_{22} \end{bmatrix} = (HL)^N \quad (8)$$

The transmission (t) and reflection (r) coefficient is obtained as:

$$\begin{aligned} t &= \frac{T}{A} = \frac{2p_1}{(m_{11} + m_{12}p_l)p_1 + (m_{21} + m_{22}p_l)} \\ r &= \frac{R}{A} = \frac{(m_{11} + m_{12}p_l)p_1 - (m_{21} + m_{22}p_l)}{(m_{11} + m_{12}p_l)p_1 + (m_{21} + m_{22}p_l)} \end{aligned} \quad (9)$$

Here, $p_1 = \sqrt{\frac{\epsilon_1}{\mu_1}} \cos \theta_1$ and $p_l = \sqrt{\frac{\epsilon_l}{\mu_l}} \cos \theta_l$

Where, ϵ_1 , μ_1 and ϵ_l , μ_l represents the electric permittivity and magnetic permeability of medium 1 and medium l respectively. The reflectivity (R) and transmissivity (T) are given as:

$$\begin{aligned} R &= |r|^2 \\ T &= \frac{p_l}{p_1} |t|^2 \end{aligned} \quad (10)$$

4. PROPOSED SENSOR DESIGN

The goal of the proposed work is to develop a theoretical design, simulation, and analysis of a distributed Bragg's mirror for the detection of thyroid cancer. When the optical thickness of these two materials is equal to quarter wavelength of the incident electro-magnetic (EM) wave then the layered structure of two different materials exhibits a high reflectivity. A cavity can be created by removing any one of the layer (low or high layer). This makes the structure to allow one particular frequency of light to propagate through it. DBR has an alternate low and high RI materials, the optical thickness of each layer is quarter wavelength of incident light. The RI of L and H layer is represented as n_L and n_H respectively. The selected materials used for L and H layers are ZnS and Ge respectively. Silicon material is used as a base material over which this multilayer structure can be grown. Light incident on this layered structure undergoes multiple reflections in this media. The incident light is normal to the structure and is TE polarized. With the introduction of defect cavity in the middle layer of DBR structure, a sharp transmission of electromagnetic wave can be observed in the stopband region. Figure 3 shows the structure of defected multilayer cavity. A central cavity is sandwiched between $N = 6$ layer on either side.

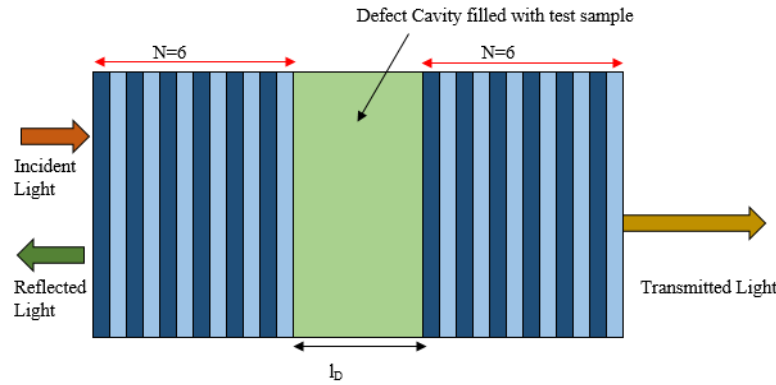


Figure 3. Proposed fabry perot microcavity with two bragg's mirror on either side with $N = 3$

Above structure can be mathematically written as [27].

$$M = \begin{bmatrix} M_a & M_b \\ M_c & M_d \end{bmatrix} = (M_H M_L)^N M_D (M_H M_L)^N \quad (11)$$

Where, M_L , M_H and M_D represents L , H , and D layer the characteristic matrix respectively.

The defect layer geometrical thickness is iterated carefully and finally chosen as $4 \mu\text{m}$. The transmission of resonant mode through the cavity is observed clearly for the normal and cancerous cells. In this work, the proposed micro-cavity structure is used to fill sample under test. The presence of thyroid cancerous cells can be detected based on the resonating wavelength of the light through the structure as soon as the sample is available at the central defect cavity. With the test sample in the central defect cavity, the incident light changes its resonating wavelength and there is a considerable wavelength shift for normal and cancerous cells. Hence, the presence of thyroid cancer cells can be detected in the given sample. In recent years, RI based detection is the widely used technique for the detection of cancerous cells. In this work, the RI of normal cells is taken as 0.8 and that of cancerous cells is taken as 0.9 [28]. From this data it is clear that the RI of cancerous cells is higher than that of normal cells.

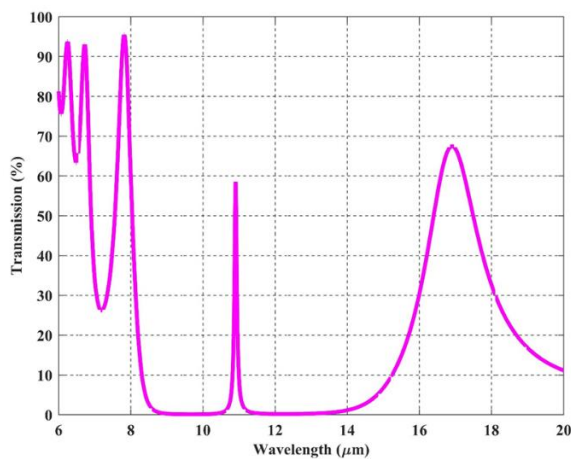


Figure 4. Normal cell transmission spectrum

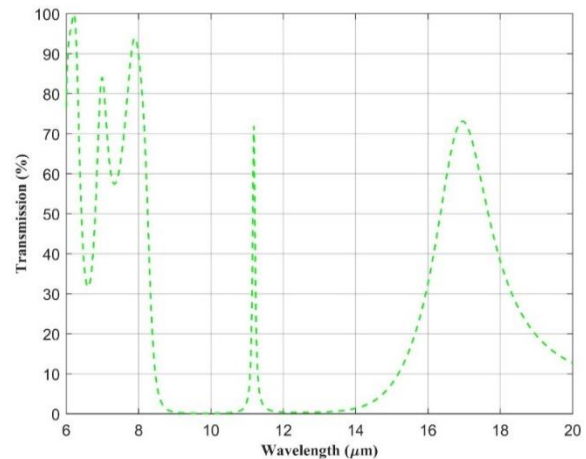


Figure 5. Thyroid cancer cell transmission spectrum

As the incident light interacts with the sample in the central cavity and resonate with certain frequency. The presence and absence of thyroid cancer cells can be distinguished by observing this resonant frequency shift. The resonance spectrum for normal and cancerous cells is as shown in the Figure 4 and Figure 5 respectively. There is a significant shift between these two spectrum as shown in the figures.

The resonant frequency of normal cell is $10.9042 \mu\text{m}$ and that of cancerous cell is $11.187 \mu\text{m}$. This shift in the resonant wavelength calculated to determine the presence of cancerous cells in the given test sample. The wavelength shift is significant and is $0.2828 \mu\text{m}$.

In Table 1, we have shown the refractive index of normal and thyroid cancer cells [28]. The value of refractive index for normal cells is less than thyroid cancer cells. As in beginning of cancer, the deposition of protein particle in cells is starts so the value of refractive index of cells become larger. Also, the value of the refractive index of final stage cancer is larger than initial stage cancer. When the defect cavity is filled with the analyte containing cancerous and normal cells there is a significant shift in the resonating wavelength as shown in the combined Figure 6. Shift in the resonating wavelength for cancer and normal cells can be measured easily.

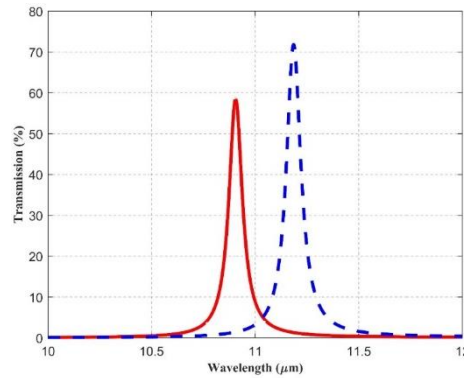


Figure 6. Combined transmission spectrum of normal and thyroid cancerous cells

Table 1. Refractive index of normal and thyroid cancer cells [28]

Cells under consideration	Refractive index (RI)
Normal	0.8
Cancerous	0.9

5. SENSOR PARAMETERS

The performance and accuracy of the sensor are the important parameters of sensor for sensing applications. Here, we have calculated two major sensor parameters like sensitivity and quality factor [12], [13]. Both parameters such as sensitivity and quality factor are most important as sensor design point of view, so we calculate both parameters in this research work and tabulated in Table 2. The sensitivity of proposed biosensor is 2.828 ($\mu\text{m}/\text{RIU}$) and Q factor is 3729.

5.1. Sensitivity

The sensing quality of a sensor is measured by using sensitivity of the sensor and is the ratio of resonant wavelength change to RI change of the sample. This is an important parameter of an optical sensor which describes the capability of the sensor to detect the desired component in a sample.

$$S_{RI} = \frac{\Delta\lambda_{res}}{\Delta n} \quad (12)$$

5.2. Quality factor

It is the ability of the sensor to detect malignant cells in the test sample. It is the ratio of resonant wavelength shift to the full width half maximum (FWHM) of a transmission spectrum. Q factor of an optical sensor describes the accuracy with which the desired component of an analyte can be measured.

$$Q = \frac{\lambda_{res}}{\lambda_{1/2}} \quad (13)$$

Table 2. Proposed biosensor performance parameters

RI of normal cells	RI of thyroid cells	Sensitivity ($\mu\text{m}/\text{RIU}$)	Q factor
0.8	0.9	2.828	3729

In order to justify the sensing ability of the proposed sensor, comparison table is shown in Table 3. It is clear from the table data that, the proposed sensor is having good sensing ability and Q factor as compared with the recently proposed works. So, in this way we can say that proposed sensor will give the better results than other sensors.

Table 3. Comparing proposed sensor with the recently reported works

Serial number	Sensor design	Sensitivity (nm/RIU)	Q factor	Reference
1	1D nano composite PhC [2019]	43	–	[29]
2	Ultra-sensitive PhC sensor [2019]	2200	10 ⁵	[27]
3	Square lattice defect-based PCW sensor [2020]	2360.12	99.765	[30]
4	Proposed work	2828	3729	–

6. CONCLUSION

A theoretical design of one-dimensional Bragg's reflector micro-cavity structure is proposed for the detection of thyroid cancer cells in the given test sample. For better sensor sensitivity an incident light is chosen in the mid-infrared range of frequency. On either side of the central defect cavity, 3 pairs of alternate low and high RI layers are present. Refractive index of normal and thyroid cancer cells is used to measure the sensor performance. The defect is filled with test sample and analysed the interaction of incident light with the sample. The resonant shift in wavelength for these cells is measured. The presence of thyroid cancerous cells is detected based on this wavelength shift. The sensor shows good Q factor and sensitivity of 3729 and 2828 nm/RIU. Obtained results concludes that the proposed sensor can be suitable for medical applications for the quick and accurate detection of thyroid cancer cells.




REFERENCES

- [1] Q. T. Nguyen, E. J. Lee, M. G. Huang, Y. I. Park, A. Khullar, and R. A. Plodkowski, "Diagnosis and treatment of patients with thyroid cancer," *Am Health Drug Benefits*, vol. 8, no. 1, pp. 30–40, 2015. [Online]. Available: <https://www.ncbi.nlm.nih.gov/pmc/articles/PMC4415174/pdf/ahdb-08-030.pdf>
- [2] E. Tokuda *et al.*, "Phosphatidylinositol 4-phosphate in the golgi apparatus regulates cell-cell adhesion and invasive cell migration in human breast cancer," *Cancer Research*, vol. 74, no. 11, pp. 3054–3066, 2014, doi: 10.1158/0008-5472.CAN-13-2441.
- [3] A. C. Schroeder and M. L. Privalsky, "Thyroid hormones, T3 and T4, in the brain," *Frontier in Endocrinology*, vol. 5, 2014, doi: 10.3389/fendo.2014.00040.
- [4] K. Sugimoto and K. Mori, "Thyroid-Stimulating Hormone Regulation and Transcription in Hypothyroidism," *Hypothyroidism - Influences and Treatments*, 2012, doi: 10.5772/32002.
- [5] G. Khan, T. Ghaffar, I. Ahmed, F. Ullah, R. Khan, and A. U. H. Aamir, "Thyroid dysfunction in patients with type 1 diabetes," *Journal of Postgraduate Medical Institute*, vol. 33, no. 2, pp. 113–116, 2019. [Online]. Available: <https://jpmi.org.pk/index.php/jpmi/article/view/2315/2262>
- [6] Y. Rochlani, N. V. Pothineni, S. Kovelamudi, and J. L. Mehta, "Metabolic syndrome: pathophysiology, management, and modulation by natural compounds," *Therapeutic Advances in Cardiovascular Disease*, vol. 11, no. 8, pp. 215–225, 2017, doi: 10.1177/1753944717711379.
- [7] "The American thyroid association," *Endocrinology*, vol. 116, no. 2, 1985, doi: 10.1210/endo-116-2-566.
- [8] D. Grimm, "Recent Advances in Thyroid Cancer Research," *International Journal of Molecular Sciences*, vol. 23, no. 9, 2022, doi: 10.3390/ijms23094631.
- [9] R. B. Gowda, P. Vanishree, and P. Sharan, "An Efficient Low Power MEMS-Based Microfluidic Device for the Segregation of Different Blood Components," *Advances in VLSI, Signal Processing, Power Electronics, IoT, Communication and Embedded Systems*, Singapore: Springer, 2021, vol. 752, pp. 39–54, doi: 10.1007/978-981-16-0443-0_4.
- [10] R. Mathias, A. P. Ambalgi, and A. M. Upadhyaya, "Grating based pressure monitoring system for subaquatic application," *International Journal of Information Technology*, vol. 10, pp. 551–557, 2018. [Online]. Available: <https://link.springer.com/article/10.1007/s41870-018-0128-x>
- [11] S. Kulkarni, N. Khan, P. Sharan and B. Ranjith, "Bacterial Analysis of Drinking Water using Photonic Crystal based Optical Sensor," *2020 7th International Conference on Computing for Sustainable Global Development (INDIACom)*, 2020, pp. 186–191, doi: 10.23919/INDIACom49435.2020.9083711.
- [12] R. B. Gowda, M. S. Manna, Saara K., and P. Sharan, "Detection of Plasmodium Falciparum Parasite Intraerythrocytic Stages using One Dimensional Distributed Bragg Reflector Biosensor," *2021 IEEE 9th Region 10 Humanitarian Technology Conference (R10-HTC)*, 2021, pp. 1–6, doi: 10.1109/R10-HTC53172.2021.9641586.
- [13] R. B. Gowda, K. Saara, and P. Sharan, "Detection of oral cancerous cells using highly sensitive one-dimensional distributed Bragg's Reflector Fabry Perot Microcavity," *Optik*, vol. 244, 2021, doi: 10.1016/j.ijleo.2021.167599.
- [14] G. Guida, A. D. Lustrac, and A. C. Priou, "An Introduction to Photonic Band Gap (PBG) Materials," *Progress in Electromagnetics Research*, vol. 41, pp. 1–20, 2003, doi: 10.2528/PIER02010801.
- [15] X. Tao, "Wearable photonics based on integrative polymeric photonic fibres," in *Wearable Electronics and Photonics*, Woodhead Publishing Limited, 2005, pp. 136–154, doi: 10.1533/9781845690441.136.
- [16] S. A. Taya, "Ternary photonic crystal with left-handed material layer for refractometric application," *Opto-Electronics Review*, vol. 26, no. 3, pp. 236–241, 2018, doi: 10.1016/j.opelre.2018.05.002.
- [17] J. N. Winn, Y. Fink, S. Fan, and J. D. Joannopoulos, "Omnidirectional reflection from a one-dimensional photonic crystal," vol. 23, no. 20, pp. 1573–1575, 1998, doi: 10.1364/OL.23.001573.
- [18] S. A. Taya, and S. A. Shaheen, "Binary photonic crystal for refractometric applications (TE case)," *Indian Journal of Physics*, vol. 92, pp. 519–527, 2018, doi: 10.1007/s12648-017-1130-z.
- [19] V. E. Rogalin, I. A. Kaplunov, and G. I. Kropotov, "Optical Materials for the THz Range," *Optics and Spectroscopy*, vol. 125, pp. 1053–1064, 2018, doi: 10.1134/S0030400X18120172.
- [20] M. Rubin, K. V. Rotkay, and R. Powles, "Window optics," *Solar Energy*, vol. 62, no. 3, pp. 149–161, 1998, doi: 10.1016/S0038-092X(98)00010-3.
- [21] R. S. Dubey and V. Ganesan, "Fabrication and characterization of TiO₂ / SiO₂ based Bragg reflectors for light trapping applications," *Results in Physics*, vol. 7, pp. 2271–2276, 2017, doi: 10.1016/j.rinp.2017.06.041.
- [22] I. -W. Feng, S. Jin, J. Li, J. Lin, and H. Jiang, "SiO₂ / TiO₂ distributed Bragg reflector near 1 . 5 1 m fabricated by e-beam




- evaporation,” *Journal of Vacuum Science & Technology*, 2013, doi: 10.1116/1.4823705.
- [23] V. Yepuri, R. S. Dubey, and B. Kumar, “Rapid and economic fabrication approach of dielectric reflectors for energy harvesting applications,” *Scientific Reports*, vol. 10, 2020, doi: 10.1038/s41598-020-73052-w.
- [24] T. Hemati and B. Weng, “The Mid-Infrared Photonic Crystals for Gas Sensing Applications,” in *Photonic Crystals - A Glimpse of the Current Research Trends*, London, United Kingdom: IntechOpen, 2018, doi: 10.5772/intechopen.80042.
- [25] A. B. Seddon, “A Prospective for New Mid-Infrared Medical Endoscopy Using Chalcogenide Glasses,” *International Journal of Applied Glass Science*, vol. 2, no. 3, pp. 177–191, 2011, doi: 10.1111/j.2041-1294.2011.00059.x.
- [26] R. B. Gowda, H. N. Gayathri, P. Sharan, and K. Saara, “Theoretical investigation of Bragg Reflector optical sensor for the measurement of cryogenic temperature,” *Material Today Proceeding*, 2022, vol. 58, pp. 451–455, doi: 10.1016/j.matpr.2022.02.482.
- [27] A. H. Aly and Z. A. Zaky, “Ultra-sensitive photonic crystal cancer cells sensor with a high-quality factor,” *Cryogenics*, vol. 104, 2019, doi: 10.1016/j.cryogenics.2019.102991.
- [28] M. R. Konnikova *et al.*, “Malignant and benign thyroid nodule differentiation through the analysis of blood plasma with terahertz spectroscopy,” *Biomedical Optics Express*, vol. 12, no. 2, pp. 1020-1035, 2021, doi: 10.1364/boe.412715.
- [29] N. R. Ramanujam *et al.*, “Enhanced sensitivity of cancer cell using one dimensional nano composite material coated photonic crystal,” *Microsystem Technologies*, vol. 25, pp. 189–196, 2019, doi: 10.1007/s00542-018-3947-6.
- [30] A. Panda and P. P. Devi, “Photonic crystal biosensor for refractive index based cancerous cell detection,” *Optical Fiber Technology*, vol. 54, 2020, doi: 10.1016/j.yofte.2019.102123.

BIOGRAPHIES OF AUTHORS






Ranjeet Kumar Pathak    received the B.Tech. degree in applied electronics and instrumentation engineering from UPTU University, SIET Greater Noida, India. In 2008, and M. Tech degree in Power Electronics and ASIC design from MNNIT, Prayagraj in 2013. Currently pursuing Ph.D. degree in electronics and communication engineering from Amity University Uttar Pradesh, Lucknow campus, Lucknow, India. He is currently Assistant Professor with the department of electronics and communication, United College of Engineering and Research, Prayagraj, UP, India. His current research interests include photonic sensor, bio-photonic sensor and machine learning. He can be contacted at email: pathak84@yahoo.co.in or ranjeet.pathak@student.amity.edu.



Sumita Mishra    received M.Tech. degree in optical communication from the Shri Govindram Seksaria Institute of Technology and Science, Indore, India, and Ph.D. degree from Dr. Ram Manohar Lohia Avadh University, Faizabad, India. She is currently Assistant Professor with the Department of Electronics and Communication Engineering, Amity School of Engineering and Technology, Amity University, Lucknow Campus. Dr. Mishra is Senior Member of IEEE, member IET (UK), IAENG and IACSIT. Her current research interests include machine learning, visible light communication and photonics. She can be contacted at email: smishra3@lko.amity.edu.



Preeti Sharan    received the Post Doctorate degree from the Indian Institute of Technology (IIT) Kharagpur, Kharagpur, India, in 2002, and the Ph.D. degree from IIT Varanasi, Varanasi, India, in 1998. She is currently a Professor with the Department of Electronics and Communication Engineering, The Oxford College of Engineering, Bangalore, India. She has received many awards, including the Young Achiever’s Award from the Karnataka Krishik Sangh in 2012, the JRF/SRF Award from the University Grants Commission, India, and the R10 IEEE Humanitarian Challenge Award from Asia Pacific in 2012 and 2013. She was a Sight Coordinator of the IEEE Bangalore Section in 2012. She has been an EXECOM Member of the Photonic Society, IEEE Bangalore Section, since 2010. She has distinction of delivering projects for prestigious funding agencies across the world: The Naval Research Board, Defence Research and Development Organisation, the IEEE USA, and the Vision Group on Science and Technology, Government of Karnataka. She has several publications in international journals and prestigious conferences. She is guiding several Ph.D. students in the research areas of integrated optics, photonic crystal sensor, optical fiber communication, and optical networking. She can be contacted at email: sharanpreeta@gmail.com.